

# Plants and mycorrhizal symbionts acquire substantial soil nitrogen from gaseous ammonia transport

Rachel Hestrin<sup>1,2</sup> , Peter K. Weber<sup>2</sup> , Jennifer Pett-Ridge<sup>2</sup>  and Johannes Lehmann<sup>1,3,4</sup> 

<sup>1</sup>Soil and Crop Sciences, School of Integrative Plant Science, Cornell University, Ithaca, NY 14853, USA; <sup>2</sup>Lawrence Livermore National Laboratory, Physical and Life Science Directorate, Livermore, CA 94550, USA; <sup>3</sup>Cornell Atkinson Center for Sustainability, Cornell University, Ithaca, NY 14853, USA; <sup>4</sup>Institute for Advanced Study, TU München, Garching 85748, Germany

## Summary

- Nitrogen (N) is an essential nutrient that limits plant growth in many ecosystems. Here we investigate an overlooked component of the terrestrial N cycle – subsurface ammonia (NH<sub>3</sub>) gas transport and its contribution to plant and mycorrhizal N acquisition.
- We used controlled mesocosms, soil incubations, stable isotopes, and imaging to investigate edaphic drivers of NH<sub>3</sub> gas efflux, track lateral subsurface N transport originating from <sup>15</sup>NH<sub>3</sub> gas or <sup>15</sup>N-enriched organic matter, and assess plant and mycorrhizal N assimilation from this gaseous transport pathway.
- NH<sub>3</sub> is released from soil organic matter, travels belowground, and contributes to root and fungal N content. Abiotic soil properties (pH and texture) influence the quantity of NH<sub>3</sub> available for subsurface transport. Mutualisms with arbuscular mycorrhizal (AM) fungi can substantially increase plant NH<sub>3</sub>-N uptake. The grass *Brachypodium distachyon* acquired 6–9% of total plant N from organic matter-N that traveled as a gas belowground. Colonization by the AM fungus *Rhizophagus irregularis* was associated with a two-fold increase in total plant N acquisition from subsurface NH<sub>3</sub> gas.
- NH<sub>3</sub> gas transport and uptake pathways may be fundamentally different from those of more commonly studied soil N species and warrant further research.

Author for correspondence:  
Johannes Lehmann  
Email: CL273@cornell.edu

Received: 6 April 2021  
Accepted: 20 May 2021

*New Phytologist* (2021) **231**: 1746–1757  
doi: 10.1111/nph.17527

**Key words:** ammonia (NH<sub>3</sub>), arbuscular mycorrhizal fungi, nitrogen (N), plant, soil.

## Introduction

Nitrogen (N) availability influences biological diversity, climate, and net primary productivity worldwide (Vitousek & Howarth, 1991; Galloway *et al.*, 2008). Our understanding of the factors that govern subsurface N transformations, transport, and biological uptake influence climate models and land management recommendations (Fowler *et al.*, 2013). However, gaps in our understanding of the N cycle continue to pose significant global challenges. For example, in agricultural systems, sufficient N is necessary for plant growth, but excessive or poorly-timed N applications can result in eutrophication, greenhouse gas emissions, and a complex cascade of environmental responses (Vitousek & Howarth, 1991; Galloway *et al.*, 2004, 2008). Despite N's critical role in the biosphere and extensive research on N cycling and management, uncertainties in estimates of N stocks and fluxes often exceed ±30–50% (Galloway *et al.*, 2004; Sutton *et al.*, 2013). This wide-ranging uncertainty is partially due to an incomplete mechanistic understanding of the N cycle, including the processes that govern plant N acquisition (Pajares & Bohannon, 2016; Moreau *et al.*, 2019).

Nonleguminous plants are thought to primarily acquire N through root uptake of ammonium (NH<sub>4</sub><sup>+</sup>) or nitrate (NO<sub>3</sub><sup>-</sup>) ions (supplied through mineral or organic fertilization,

atmospheric deposition, or as decomposition products of organic matter), as well as some amount from small organic molecules or through mutualistic interactions with soil organisms (Chapin *et al.*, 1993; Näsholm *et al.*, 1998; Leigh *et al.*, 2009; Huygens *et al.*, 2016; Chalk & Smith, 2020). Plants also take up a variety of other N species (such as NO<sub>y</sub> and ammonia (NH<sub>3</sub>) gas) through their aerial tissues, with significant implications for the net balance and isotopic composition of plant-assimilated N, ecological interactions, atmospheric chemistry, and global N budgets (Farquhar *et al.*, 1980; Schjoerring *et al.*, 2000; Sparks *et al.*, 2001; Riedo *et al.*, 2002; van Hove *et al.*, 2002; Johnson & Berry, 2013; Campbell & Vallano, 2018). Studies that investigate root acquisition of these N species remain relatively uncommon. However, widespread use of anhydrous NH<sub>3</sub> fertilizer provides empirical evidence that roots can acquire substantial quantities of N from subsurface NH<sub>3</sub> gas. NH<sub>3</sub> gas may also be a relevant source of plant N in unfertilized systems; soils under natural vegetation release more than 2.4 Tg NH<sub>3</sub>-N yr<sup>-1</sup> to the atmosphere, with some estimates reaching an order of magnitude more (Dawson, 1977; Dentener & Crutzen, 1994; Bouwman *et al.*, 1997; Bouwman *et al.*, 2002; Ciais *et al.*, 2013; Sutton *et al.*, 2013). If this quantity of NH<sub>3</sub> gas is released from soil to the atmosphere, we hypothesize that a substantial quantity of subsurface NH<sub>3</sub> is transformed or intercepted by plants or microbes beforehand.

It is typically assumed that  $\text{NH}_3$  gas is either rapidly volatilized or protonated into  $\text{NH}_4^+$  ions that can be taken up by plants or microbes, nitrified, or adsorbed to soil particles, but remain relatively immobile. If instead, subsurface  $\text{NH}_3$  persists as a gas, its movement and contribution to plant nutrition would likely follow different spatial and temporal patterns compared to  $\text{NH}_4^+$  ions or other more commonly studied soil N species. Several variables influence subsurface  $\text{NH}_3$  gas production and transport, including substrate availability, moisture, temperature, pH, soil texture, and microbial activity (McCalley & Sparks, 2008; Flechard *et al.*, 2013; Pelster *et al.*, 2019). These ecological variables likely mediate the degree to which  $\text{NH}_3$  gas contributes to plant N nutrition. Plant–microbe relationships that enhance plant nutrition may also influence plant acquisition of N from  $\text{NH}_3$  gas. Arbuscular mycorrhizal (AM) fungi can increase plant N acquisition from both organic and inorganic sources, with implications for plant productivity, organic matter dynamics, and soil N cycling (Mader *et al.*, 2000; Hodge *et al.*, 2001; Leigh *et al.*, 2009; Hodge & Fitter, 2010; Hestrin *et al.*, 2019). However, no studies have explicitly investigated AM acquisition of  $\text{NH}_3$ -N or subsequent N transfer to plants.

In a series of previous experiments with the model grass *Brachypodium distachyon* and the AM fungus *Rhizophagus irregularis* (formerly *Glomus intraradices*), we observed that plants assimilated organic matter-derived N, even under conditions that precluded direct contact with the organic matter and indirect access to N through microbial transport, aqueous diffusion, or mass flow. Plants inoculated with the AM fungus assimilated more organic matter-derived N than uninoculated plants, even when the fungus was also excluded from compartments containing the organic matter. Combined with our observation that plants took up more of this organic matter-derived N under alkaline conditions (which favor the presence of  $\text{NH}_3$  gas rather than protonated  $\text{NH}_4^+$  ions), these results led us to hypothesize that as the organic matter decomposed, it released  $\text{NH}_3$  gas that diffused belowground and was taken up by plant roots and their mycorrhizal partners. Although stomatal  $\text{NH}_3$  uptake can constitute several percent of total assimilated plant N, subsurface  $\text{NH}_3$  gas exchange through root tissues is rarely considered (Farquhar *et al.*, 1980; Schjoerring *et al.*, 2000; Riedo *et al.*, 2002; van Hove *et al.*, 2002; Gruber & Galloway, 2008; Ciais *et al.*, 2013; Johnson & Berry, 2013; Zhu *et al.*, 2016; Weil & Brady, 2017) and AM fungal  $\text{NH}_3$  uptake has never been investigated. Therefore, we sought to assess whether N that originates as  $\text{NH}_3$  gas could travel laterally belowground and contribute to plant and fungal N nutrition, and to what extent edaphic properties influence the quantity and mobility of  $\text{NH}_3$  that might be available for this pathway.

## Materials and Methods

### Plant and fungal propagation

*Brachypodium distachyon* seeds were surface sterilized with ethanol and planted in cones (Ray Leach Cone-tainers; Stuewe & Sons Inc., Tangent, OR, USA) filled with 1:1 mixtures of

double-autoclaved sand and gravel (v/v) at neutral pH. For AM fungal inoculation, 500 spores of the AM fungus *R. irregularis* (previously *G. intraradices*) were added at the time of seeding (Hong *et al.*, 2012). Plant and fungal mesocosms were maintained in a growth chamber set to a 12 h photoperiod with temperatures of 24°C during the day and 22°C at night (Percival AR-100L3; Percival Systems Inc., Perry, IA, USA). After *c.* 1 month, plants were transplanted from cones into mesocosms containing 1:1 mixtures of double-autoclaved sand and gravel (v/v) at neutral pH (see later for more detail regarding mesocosm design). Surface-sterilized seeds and autoclaved sand:gravel mixtures were used in order to minimize the presence of microorganisms and N availability in the mesocosms (Hodge *et al.*, 2001; Dijkstra *et al.*, 2010; Nuccio *et al.*, 2013). Additionally, the mesocosms were watered only with reverse osmosis filtered water and kept in a growth chamber inside a limited-access plant growth facility. However, the growing conditions were not completely sterile and some microbes may have been introduced into the mesocosms over the course of the experiment. To sustain plant growth over the course of a growing season, plants were fertilized with a low-N modified Hoagland's solution (0.5 mM KCl, 0.5 mM  $\text{CaCl}_2$ , 0.5 mM  $\text{Ca}(\text{NO}_3)_2$ , 0.5 mM  $\text{KNO}_3$ , 1 mM  $\text{MgSO}_4$ , 50  $\mu\text{M}$  NaFe EDTA, 20  $\mu\text{M}$   $\text{KH}_2\text{PO}_4$ , 10  $\mu\text{M}$   $\text{H}_3\text{BO}_3$ , 0.2  $\mu\text{M}$   $\text{Na}_2\text{MoO}_4$ , 1  $\mu\text{M}$   $\text{ZnSO}_4$ , 2  $\mu\text{M}$   $\text{MnCl}_2$ , 0.5  $\mu\text{M}$   $\text{CuSO}_4$ , 0.2  $\mu\text{M}$   $\text{CoCl}_2$ , 25  $\mu\text{M}$  HCl, and 0.5 mM MES buffer). The mesocosms were watered regularly to provide sufficient water for plant growth without saturating the sand:gravel mixture.

### Three-compartmented mesocosms

Three-compartmented mesocosms were used to track  $^{15}\text{NH}_3$  gas movement through subsurface substrates and subsequent  $^{15}\text{N}$  uptake by plant roots and AM fungi (Fig. 1a). Mesocosms were made from plastic divider boxes (Uline, Chicago, IL, USA) and rigid polypropylene dividers (United States Plastics Corp., Lima, OH, USA). Each mesocosm contained a plant compartment at one end, a compartment for pH-adjusted sand in the middle (pH 4, 7 or 10), and a compartment for gas injection fitted with a septum at the other end. Approximately 1 month after germination (see earlier), seedlings were transplanted into the plant compartment and grown for another 4 months in a 1:1 mixture of double-autoclaved sand and gravel (v/v) at neutral pH. Plants were fertilized biweekly with a modified Hoagland's solution (see earlier), which supplied a total of 11.5 mg N. After a total of 5 months of growth, the middle compartment of each mesocosm was filled with a sand substrate adjusted to a pH of either 4, 7 or 10 through repeated rinsing with deionized water ( $\text{diH}_2\text{O}$ ) or a combination of  $\text{diH}_2\text{O}$  and 1 M hydrochloric acid (HCl) until the desired pH was reached. Dividers separating the plant and pH-adjusted compartment were fitted with windows of polyester felt with 1  $\mu\text{m}$  openings to allow gas diffusion but prevent fungal and root growth into the middle compartment containing the pH-adjusted substrate. A full factorial design crossing AM colonization (two levels: –AM and +AM) with the pH of the substrate

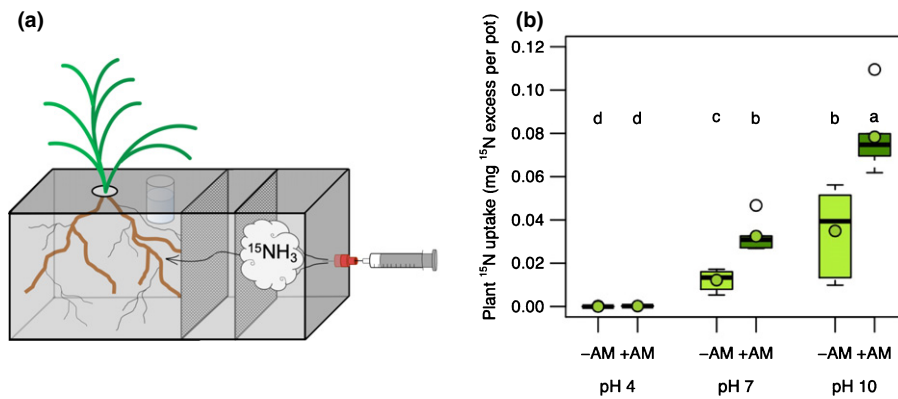


**Fig. 1** Subsurface plant acquisition of  $\text{NH}_3\text{-N}$ . (a) Three-compartmented mesocosms were used to track subsurface  $^{15}\text{NH}_3$  movement and acquisition by plant roots (*Brachypodium distachyon*) and arbuscular mycorrhizal (AM) fungi (*Rhizophagus irregularis*). Each mesocosm contained a plant compartment at one end, a compartment for pH-adjusted sand substrate in the middle (pH 4, 7 or 10), and a compartment for gas injection fitted with a septum at the other end. (b) Subsurface plant  $^{15}\text{N}$  uptake from  $^{15}\text{NH}_3$  gas is enhanced by alkaline substrate pH and mycorrhizal colonization. Bold black lines represent the median values; circles represent the mean values; whiskers represent the upper and lower quartiles ( $n = 6$  replicates per treatment). Letters denote the results of a Tukey's HSD test performed on log-transformed data ( $P < 0.05$ ).

separating the plant from the gas injection compartment (three levels: pH 4, 7 and 10) resulted in six experimental treatments, each of which was replicated six times.

Immediately following the addition of the pH-adjusted substrate, mesocosms were covered with tight-fitting lids and 20 ml of a 5%  $^{15}\text{NH}_3$  gas mixture (98 at%  $^{15}\text{NH}_3$  in a balance of 95%  $\text{N}_2$  at natural isotopic abundance) were injected into the gas injection compartment (AirLiquide, Plumsteadville, PA, USA). To assess whether plants were able to assimilate  $^{15}\text{NH}_3$  through their aerial tissues, six control mesocosms were evenly distributed amongst the rest of the mesocosms and did not receive an injection of  $^{15}\text{NH}_3$  gas. Traps containing 2% boric acid placed at the substrate surface in the plant compartment were also used to prevent  $^{15}\text{NH}_3$  gas from escaping from the subsurface into the atmosphere, where it might have been possible for aerial plant tissues to assimilate this gaseous N. Additionally, an airflow rate of 40 cubic feet per minute was maintained throughout the 3-d  $^{15}\text{NH}_3$  exposure period to homogenize the atmosphere surrounding the mesocosms and distribute any potential escaping  $^{15}\text{NH}_3$  gas evenly across all mesocosms. Three days after  $^{15}\text{NH}_3$  gas injection, to further limit the likelihood of  $^{15}\text{NH}_3$  uptake through aboveground tissues, 2% boric acid was injected through the gas injection compartment septa into empty vials inside in order to capture any remaining  $^{15}\text{NH}_3$  gas that had not traveled through the mesocosm. After the 2% boric acid was injected, plant aboveground and belowground tissues, fungi, and subsurface substrate samples were collected. Plant tissues were dried at  $50^\circ\text{C}$  for 48 h and milled into a fine powder. Fungal hyphae were harvested by floating hyphal fragments out of soil samples (Hestrin *et al.*, 2019). Briefly, 30 g of subsurface substrate were agitated vigorously in 100 ml water. After 2 min, the substrate was allowed to settle for 30 s and the solution was decanted and filtered through 10- $\mu\text{m}$  nylon filters. Large particulate matter was removed, remaining hyphal fragments were rinsed thoroughly with water, and fragments were dried as described earlier. Isotope ratio mass spectrometry (IRMS) was used to measure the

total N and isotopic composition of the milled samples (Thermo Scientific Delta V Isotope Ratio Mass Spectrometer coupled to a Carlo Erba NC2500 Elemental Analyzer).

## Two-compartmented mesocosms

Two-compartmented mesocosms were used to assess whether N from  $^{15}\text{N}$ -enriched organic matter could travel below ground in gaseous form and be acquired by plants (Fig. 2a). Treatments included mycorrhizal colonization (-AM or +AM, each replicated five times). Each mesocosm consisted of a plant compartment containing a 1 : 1 mixture of double-autoclaved sand and gravel (v/v) at neutral pH and a smaller compartment containing 1 g  $^{15}\text{N}$ -enriched organic matter (maize stover enriched at 366‰  $\delta^{15}\text{N}$ ) mixed with double-autoclaved sand. The organic matter compartment was fully enclosed, aside from a window consisting of a hydrophobic gas-permeable membrane (polytetrafluoroethylene (PTFE) unlaminate membrane filter; Sterlitech Corporation, Kent, WA, USA) on one side and stainless-steel mesh with 43  $\mu\text{m}$  openings on the other side of an air gap (325 Mesh T304 Stainless; TWP Inc., Berkeley, CA, USA). This double-paned window allowed gases to travel from the organic matter into the plant compartment, but restricted aqueous mass flow, ion diffusion through water, and direct root and hyphal access to the  $^{15}\text{N}$ -enriched organic matter. A 2% boric acid trap was placed at the surface of the organic matter compartment, which was covered with a lid to inhibit  $\text{NH}_3$  gas from escaping vertically into the atmosphere, where it might have been possible for aerial plant tissues to assimilate this gaseous N. Plants were fertilized biweekly with a modified Hoagland's solution (see earlier), which supplied a total of 29.4 mg N over the course of the experiment. Plant aboveground and belowground tissues were harvested 100 d after transplanting, dried at  $60^\circ\text{C}$  for 48 h, and milled into a fine powder. IRMS was used to measure the total N and isotopic composition of the milled plant tissues (Thermo Scientific Delta V Isotope Ratio Mass Spectrometer coupled to a Carlo Erba NC2500 Elemental Analyzer).

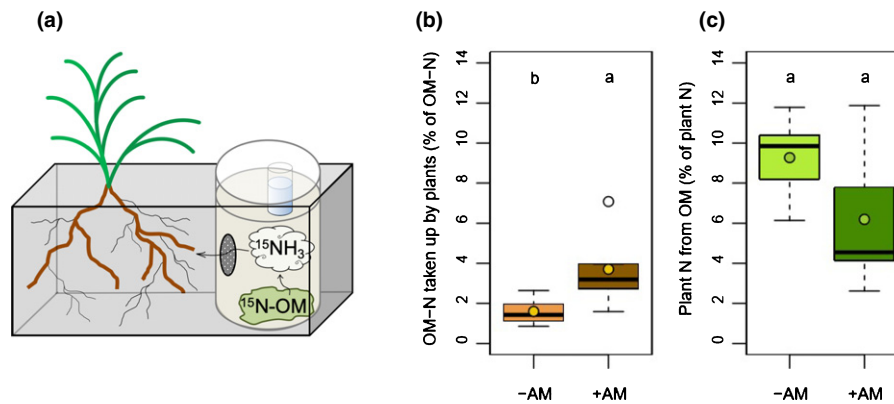


**Fig. 2** Subsurface plant acquisition of  $\text{NH}_3$ -N from organic matter. (a) Two-compartmented mesocosms were used to track subsurface gaseous  $^{15}\text{N}$  movement from organic matter and subsequent acquisition by plant roots (*Brachypodium distachyon*). Each mesocosm consisted of a plant compartment containing a smaller compartment containing  $^{15}\text{N}$ -enriched organic matter. (b, c) Nitrogen-15 ( $^{15}\text{N}$ ) released from  $^{15}\text{N}$ -enriched organic matter ( $^{15}\text{N}$ -OM) during decomposition travels in gaseous form and is taken up by plants belowground. Plants colonized by arbuscular mycorrhizal (AM) fungi take up significantly more OM-N through this pathway than uncolonized plants. (b) The proportion of total OM-N taken up by uncolonized plants and plants colonized by AM fungi is shown in light brown and dark brown boxplots, respectively ( $P < 0.05$ ). (c) The proportional contribution of OM-N to total N taken up by uncolonized and AM-colonized plants is shown in light green and dark green boxplots, respectively ( $P = 0.1077$ ). Bold black lines represent the median values; circles represent the mean values; whiskers represent the upper and lower quartiles ( $n = 5$  replicates per treatment). Letters denote the results of a Tukey's HSD test performed separately for each plot on log-transformed data ( $P < 0.05$ ).

## Nitrogen uptake calculations

**Plant nitrogen acquisition from organic matter** Plant N acquisition from organic matter was estimated based on the  $^{15}\text{N}$  content of plant tissues and on the  $^{15}\text{N}$  content of the original organic matter added to each mesocosm. The  $^{15}\text{N}$ -enriched organic matter supplied each mesocosm with  $171.669 \mu\text{g } ^{15}\text{N}$  excess. To estimate the proportion of organic matter N (including both  $^{15}\text{N}$  and  $^{14}\text{N}$ ) that plants acquired, we divided total plant tissue  $^{15}\text{N}$  excess by  $171.669 \mu\text{g}$  (Fig. 2b). This calculation assumes that plants acquired  $^{14}\text{N}$  and  $^{15}\text{N}$  at the same ratio that was initially present in the organic matter. To estimate the proportion of total plant N derived from organic matter, we divided total plant N acquired from organic matter by the total quantity of N present in plant tissues (Fig. 2c). These calculations did not account for isotopic fractionation that may occur during decomposition, or if the fungi pass the lighter N isotope to their hosts (Hobbie *et al.*, 1999; Hobbie & Högberg, 2012). However, the magnitude of such fractionation is likely small compared to the isotopic enrichment of the organic matter added. Additionally, discrimination against the heavy isotope would render our interpretation somewhat conservative in this case.

**Proportion of daily plant nitrogen acquired from subsurface ammonia gas (Supporting Information Fig. S1)** Daily plant N acquisition was estimated by dividing total plant N content by the number of growing days. To estimate the proportion of daily plant N uptake from subsurface  $\text{NH}_3$  gas, plant  $\text{NH}_3$ -N content (based on plant tissue  $^{15}\text{N}$  atom% excess, which plants derived from  $^{15}\text{NH}_3$  gas injected into the mesocosms) was divided by the average plant N uptake during a 3-d time period (the length of the  $^{15}\text{NH}_3$  exposure period). Because these plants were harvested at the end of their growing cycle (5 months) when growth rates and N uptake slow, this is likely to be an underestimate of the proportion of daily N acquired from  $\text{NH}_3$  gas during the 3-d exposure period.

## Root staining for mycorrhizal visualization

A subsample of roots from each plant was collected at harvest, fixed in 50% ethanol and stained with Trypan blue (Phillips & Hayman, 1970). Briefly, roots were cleared with 20% potassium hydroxide (KOH) at room temperature for 1 wk, acidified in 0.1 M HCl for 2 h, and stained with acidified glycerol containing 0.05% Trypan blue overnight. Mycorrhizal colonization was assessed using light microscopy and visual estimation (Giovannetti & Mosse, 1980). Colonized root segments were selected for nanoscale secondary ion mass spectrometry (NanoSIMS) imaging.

## NanoSIMS sample processing and isotope imaging

A subsample of AM-colonized roots exposed to  $^{15}\text{NH}_3$  in a three-compartmented mesocosm containing a middle compartment filled with a substrate adjusted to pH 10 was fixed in 50% ethanol and stained as described earlier. To prepare the root segment for NanoSIMS, the root was mounted onto a poly-L-lysine-coated glass slide, flattened through the application of light pressure to a coverslip temporarily laid on top of the sample, desiccated, and coated with *c.* 5 nm of gold. We collected NanoSIMS measurements at a depth of *c.* 60 nm into the sample surface. Therefore, the chemical and isotopic distributions shown in Fig. 3 represent root and fungal structures only on the exterior of the root; they do not represent the chemical or isotopic composition of the deeper intraradical fungal structures that can be visualized with light microscopy. Although sample topography can change the relative ion yield of different molecules (e.g.  $\text{CN}^-$  vs  $\text{C}^-$ ; Thomen *et al.*, 2014), the relative magnitude of this effect is small for isotopologues of the same molecule (e.g.  $^{12}\text{C}^{14}\text{N}^-$  and  $^{12}\text{C}^{15}\text{N}^-$ ; Frisz *et al.*, 2013), and therefore the effect is negligible in substantially isotopically enriched samples such as those in this study. Furthermore, we chose to collect NanoSIMS

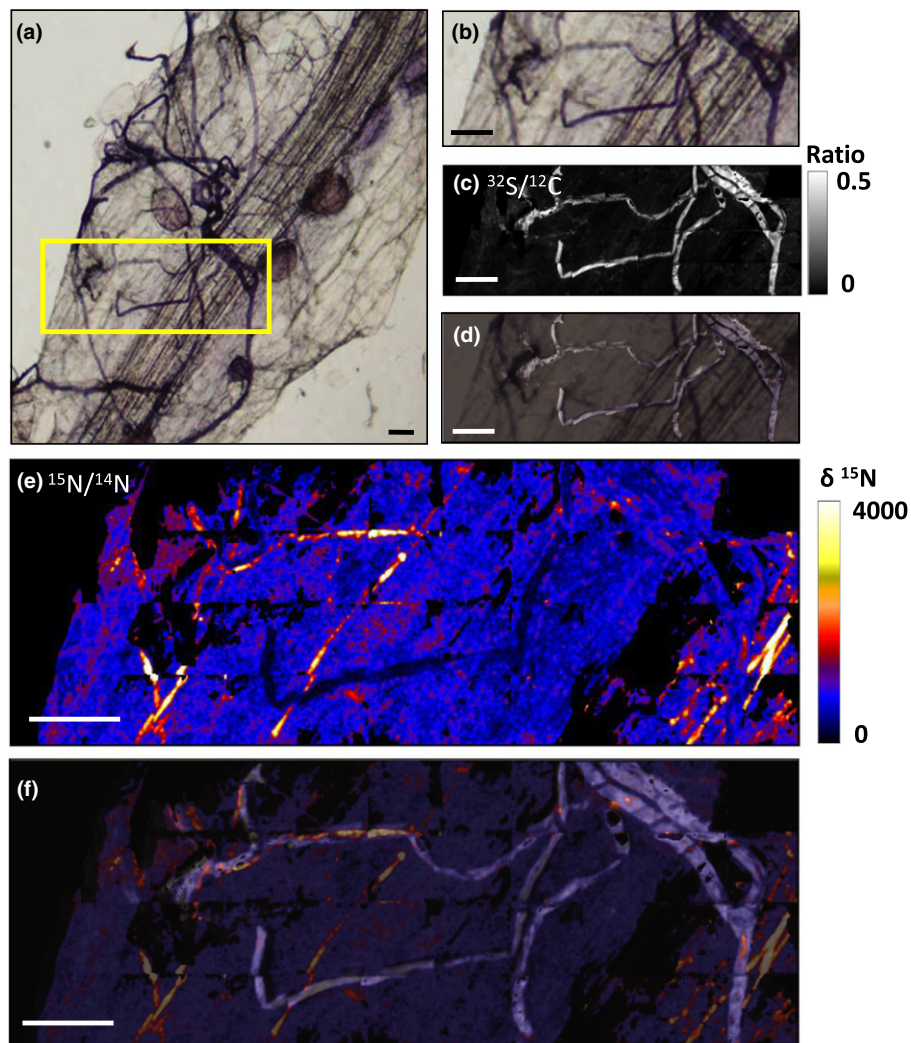


**Fig. 3** Light microscopy and nanoscale secondary ion mass spectrometry (NanoSIMS) images of a mycorrhizal root following exposure to  $^{15}\text{NH}_3\text{-N}$ . (a, b) Fungal hyphae and vesicles growing inside and around the root are stained in dark blue with acidified glycerol containing 0.05% Trypan blue. The light microscopy images show fungal structures present above the root surface and inside the root. The yellow rectangle indicates the region shown in (b)–(f) and analyzed with NanoSIMS. The NanoSIMS images show the chemical composition of the sample surface. Therefore, some of the subsurface intraradical fungal structures that can be visualized with light microscopy are not seen in (c), (e), and (f). (c) Sulfur NanoSIMS ion image collected from the same region. (d) The sulfur NanoSIMS image overlaid on top of the light microscopy image indicates which fungal structures are located on the sample surface and imaged in our NanoSIMS analysis. The partial overlap between the hyphae identified via light microscopy and those evident in the sulfur NanoSIMS image suggests: (i) the fungal tissues are enriched in sulfur compared to the plant root and (ii) some fungal structures visible by light microscopy are not detected by NanoSIMS because they are below the root surface. (e) The  $\delta^{15}\text{N}$  NanoSIMS image showing N enrichment depicted in a color scale. (f) Sulfur NanoSIMS image overlaid with the  $\delta^{15}\text{N}$  NanoSIMS image. Together, these images show that some hyphae are highly enriched with  $^{15}\text{N}$  while others are not. Bars (all panels), 50  $\mu\text{m}$ .

measurements from a contiguous flat region of our sample, thereby further minimizing potential topographic artifacts. NanoSIMS data were collected and processed as previously described (Ghosal *et al.*, 2008; Nuccio *et al.*, 2013). Briefly, imaging was performed with a CamecaNanoSIMS 50 microprobe at Lawrence Livermore National Laboratory (Livermore, CA, USA). A focused primary ion beam (2 pA, *c.* 150 nm, 16 keV  $^{133}\text{Cs}^+$ ) was used in a raster pattern with  $40 \times 40 \mu\text{m}^2$  areas of  $256 \times 256$  pixels and a dwell time of 1 ms/pixel for 20 scans. Before analysis, each raster was sputtered with 100 pA of  $\text{Cs}^+$  current to a depth of *c.* 60 nm (980 s) to reach sputtering equilibrium. Serial quantitative secondary ion images were

simultaneously collected for  $^{12}\text{C}^-$ ,  $^{12}\text{C}^{14}\text{N}^-$ ,  $^{12}\text{C}^{15}\text{N}^-$  and  $^{32}\text{S}^-$  using electron multipliers in pulse counting mode. The  $^{15}\text{N} : ^{14}\text{N}$  isotope ratio images were calculated by dividing  $^{12}\text{C}^{15}\text{N}^-$  counts by the  $^{12}\text{C}^{14}\text{N}^-$  counts on a pixel-by-pixel basis.

#### Soil incubation and measurement of net $\text{NH}_3$ and $\text{CO}_2$ efflux

To test our hypothesis that soil acidity, clay content, organic matter content, and microbial activity are associated with net  $\text{NH}_3$  efflux, we incubated 10 soils that were previously reported on and represent a range of these edaphic properties. We

measured soil pH in 2N potassium chloride (KCl) (ratio of 1 : 2 g ml<sup>-1</sup>). Other edaphic characteristics were measured and reported by authors (for more information about each soil, please see: Zackrisson *et al.*, 1996; Liang *et al.*, 2006; Solomon *et al.*, 2009; Recha *et al.*, 2012; Cayuela *et al.*, 2013; Dharmakeerthi *et al.*, 2015; Mueller *et al.*, 2015; Ahmed *et al.*, 2017). Each soil was homogenized and sieved to a particle size of 2 mm or smaller. Then, 20 g of air-dried soil were added to 60 ml glass jars and mixed with water to 60% water holding capacity. These jars were placed inside a larger glass jar with a tight-fitting lid. Each large jar also contained a 2% boric acid trap to capture NH<sub>3</sub> volatilizing from the soil and a 0.09 M KOH trap made with CO<sub>2</sub>-free water to capture CO<sub>2</sub>. Blank jars, containing NH<sub>3</sub> and CO<sub>2</sub> traps but no soil, were used to assess background levels of NH<sub>3</sub> and CO<sub>2</sub>. Eight jars were used per treatment – four replicates were harvested for an initial timepoint and four replicates were incubated in the dark at 30°C for 2 wk. At both the initial and final timepoints, NH<sub>3</sub> concentrations were measured in the boric acid traps using an ELIT NH<sub>4</sub><sup>+</sup> selective electrode (NICO 2000, Harrow, UK). In addition, the change in electrical conductivity in the KOH traps was used to assess CO<sub>2</sub> concentrations at both the initial and final timepoints (Whitman *et al.*, 2014). Mean NH<sub>3</sub> and CO<sub>2</sub> concentrations measured in blank jars were subtracted from the concentrations measured in sample jars. Daily NH<sub>3</sub> and CO<sub>2</sub> emissions were calculated by dividing the net NH<sub>3</sub> and CO<sub>2</sub> captured by the length of the incubation.

## Data analysis

All statistical analyses were performed using the LSMEANS, LME4, or LMERTEST package in the statistical computing language and environment R (R Development Core Team, 2011; Bates *et al.*, 2015). Most means comparisons were conducted using a Tukey's HSD (honest significant difference) test in the LSMEANS package. Statistical significance was assessed at either  $P < 0.05$  or  $P < 0.01$ , as indicated in the caption associated with each plot. The Tukey's HSD test compared the means for all treatments while averaging for the effect of blocking. First, a linear model was created including a fixed effect for treatment and a block effect to account for the spatially distributed randomized block design. Q-Q plots and plots of the residual vs fitted values were used to determine whether data met the assumptions of normality. If the raw data did not meet the assumptions of normality, a log transformation was applied and statistical analyses were conducted using the log-transformed data.

## Results

### Plant biomass response to arbuscular mycorrhizal fungi

Inoculation with AM fungi was associated with a two- to three-fold increase in biomass of AM-colonized plants compared to uncolonized plants in both the three-compartmented and two-compartmented mesocosms ( $P < 0.05$ , Fig. S1). The pH of the substrate in the compartment separating the plant roots from the

<sup>15</sup>NH<sub>3</sub> source in three-compartmented mesocosms had no effect on plant biomass. This was expected because the pH-adjusted substrate was added to the mesocosms immediately before the 3-d <sup>15</sup>NH<sub>3</sub> exposure period and was separated from the roots and mycorrhizal fungi by a polyester felt divider with 1 μm diameter openings. Thus, both the short exposure period and the physical separation precluded the development of a difference in plant biomass due to the presence of the pH-adjusted substrate.

### Plant nitrogen acquisition from subsurface ammonia gas

After 5 months of growth in the three-compartmented mesocosms, plant tissues contained 6.6–12.0 mg N (Fig. S2). Of this total N content, plants acquired up to 0.08 mg <sup>15</sup>N from the injected <sup>15</sup>NH<sub>3</sub> gas during the 3-d exposure period (Fig. 1b). This represents up to 0.67% of total plant N (Fig. S3) and up to 14% of the <sup>15</sup>N originally injected as <sup>15</sup>NH<sub>3</sub>. When divided by estimated plant N assimilated over the 3-d <sup>15</sup>NH<sub>3</sub> exposure period, plant <sup>15</sup>N assimilation from <sup>15</sup>NH<sub>3</sub> represents up to one-third of daily plant N assimilation (Fig. S4). Plant <sup>15</sup>N assimilation was significantly associated with the pH of the substrate separating the plants from the <sup>15</sup>NH<sub>3</sub> source ( $P < 0.05$ , Fig. 1b; Supporting Information Table S1). Plants grown in mesocosms with acidic substrate separating their roots from the <sup>15</sup>NH<sub>3</sub> source assimilated  $< 0.2 \mu\text{g } ^{15}\text{N}$  ( $< 0.04\%$  of the <sup>15</sup>N originally injected as <sup>15</sup>NH<sub>3</sub>).

### Arbuscular mycorrhizal fungal contribution to plant nitrogen acquisition from ammonia gas

Symbiotic associations with AM fungi also played a significant role in plant acquisition of NH<sub>3</sub>-derived N ( $P < 0.001$  for the overall effect of AM colonization, Table S1). When neutral or alkaline substrate separated the plants from the <sup>15</sup>NH<sub>3</sub> source, AM-colonized plants took up 0.03 and 0.08 mg <sup>15</sup>N, respectively – approximately twice as much <sup>15</sup>N as plants that were grown without AM fungi ( $P < 0.05$ , Fig. 1b). The greater total quantity of <sup>15</sup>N measured in the AM-colonized plants was due to a combination of both greater biomass of AM-colonized plants, which were over twice as large as those of uncolonized plants ( $P < 0.05$ , Fig. S1) and higher  $\delta^{15}\text{N}$  value of AM-colonized roots ( $P < 0.01$ , Fig. S5).

### NanoSIMS imaging of roots and fungal hyphae

We used NanoSIMS imaging to assess the spatial distribution of N isotopes in the surface tissue of AM-colonized roots and extraradical AM fungal hyphae following exposure to <sup>15</sup>NH<sub>3</sub>. The <sup>32</sup>S : <sup>12</sup>C ratio of fungal hyphae was higher than that of the root tissue and helps to identify the location of the extraradical fungal hyphae in the N isotope images (Fig. 3c,e,f). The <sup>15</sup>N : <sup>14</sup>N ratio image shows that AM fungal assimilation of <sup>15</sup>N from <sup>15</sup>NH<sub>3</sub> was highly heterogeneous – some hyphae were enriched beyond 4000‰  $\delta^{15}\text{N}$ , while others were not enriched (Fig. 3e,f). Root <sup>15</sup>N enrichment was also heterogeneous, containing some features that were enriched beyond 4000‰  $\delta^{15}\text{N}$ , but the

majority of the root tissue was not substantially enriched above natural isotopic abundance.

### Plant acquisition of organic matter-nitrogen transported as subsurface gas

When grown for 100 d in two-compartmented mesocosms containing  $^{15}\text{N}$ -enriched organic matter separated from roots and fungal hyphae with a hydrophobic gas-permeable membrane (see Fig. 2a for mesocosm design), plants assimilated up to 3.7% of the original N content of the organic matter (Fig. 2b). Since neither the roots nor their mycorrhizal partners had direct access to the organic matter, and the double-paned air gap prevented aqueous diffusion or mass flow, the remaining pathway for N travel between compartments was through the lateral movement of N gas. Plants colonized by AM fungi acquired more than twice the quantity of organic matter-N compared to uncolonized plants (Figs 2b, S6a,  $P < 0.05$ ). However, the proportion of total plant N that AM-colonized plants acquired from organic matter via N gas transport was lower than the proportion acquired by uncolonized plants. AM-colonized plants acquired 6.2% of their total N from organic matter after 100 d of growth, while uncolonized plants acquired 9.3% of their total N from organic matter ( $P = 0.1077$ , Fig. 2c). The  $\delta^{15}\text{N}$  values of AM-colonized plants were significantly lower than those of uncolonized plants ( $P < 0.05$ , Fig. S6b).

### Variation in ammonia efflux from natural soils

To explore abiotic factors that govern the quantity of subsurface  $\text{NH}_3$  that is available to move below ground and be acquired by plant roots and soil microorganisms, we measured  $\text{NH}_3$  efflux during a laboratory incubation of 10 well-characterized soils developed under natural vegetation. These soils represent a wide range of soil pH, clay content, carbon (C) content, and N content, which we hypothesized would be associated with  $\text{NH}_3$  efflux (Table S2; see previous studies of these soils described by Zackrisson *et al.*, 1996; Liang *et al.*, 2006; Solomon *et al.*, 2009; Recha *et al.*, 2012; Cayuela *et al.*, 2013; Dharmakeerthi *et al.*, 2015; Mueller *et al.*, 2015; Ahmed *et al.*, 2017). The range of  $\text{NH}_3$  efflux from these soils spanned an order of magnitude (Fig. S7).  $\text{NH}_3$  efflux was positively associated with soil pH and negatively associated with clay content (Fig. 4a,b,  $P < 0.01$ ,  $R^2 = 0.55$  for pH;  $P < 0.05$  and  $R^2 = 0.56$  for clay), but did not appear to be significantly associated with soil N, soil C, or  $\text{CO}_2$  efflux – a proxy for heterotrophic microbial activity (Fig. 4c–e). These results support our hypothesis that soil chemistry and mineralogy are strong mediators of  $\text{NH}_3$  efflux and subsequent availability for plant or microbial uptake. Because soil moisture and temperature mediate  $\text{NH}_3$  efflux (Potter *et al.*, 2003; McCalley & Sparks, 2008), we incubated the soils at a single temperature (30°C) and moisture level (60% water holding capacity) in order to highlight the relationship between  $\text{NH}_3$  efflux and other edaphic properties. Thus, the results presented here do not reflect  $\text{NH}_3$  efflux from other environments or under natural conditions.

## Discussion

### Ammonia gas may be an important component of subsurface nitrogen transport and biotic nitrogen acquisition

This study provides evidence for subsurface production and transport of gaseous  $\text{NH}_3$ , as well as biotic (plant and fungal) uptake of  $\text{NH}_3\text{-N}$ . Specifically, our experiments show that: (1) plants and mycorrhizal fungi acquire N that originates as  $\text{NH}_3$  gas (Figs 1, 3, S3–S5); (2) plants and mycorrhizal fungi acquire organic matter-N through a subsurface pathway that precludes direct contact, mass flow, or ion diffusion (Figs 2, S6); and (3) there is substantial variation in the quantity of subsurface  $\text{NH}_3$  that might be available for travel and biotic uptake in different soils (Figs 4, S7). Although several nitrogenous gases that originate from organic matter (such as  $\text{NH}_3$ ,  $\text{NO}$ ,  $\text{N}_2\text{O}$  or  $\text{N}_2$ ) may travel belowground and be intercepted by roots and microorganisms, we posit that  $\text{NH}_3$  is the most likely gas to contribute to subsurface inorganic N acquisition by nondiazotrophic organisms. Mineralization of organic matter to  $\text{NH}_3$  :  $\text{NH}_4^+$  precedes nitrification and denitrification to other nitrogenous gases, such as  $\text{NO}$ ,  $\text{N}_2\text{O}$  or  $\text{N}_2$  (Stein & Klotz, 2016). The  $\text{NH}_3$  gas molecules produced are immediately available for subsurface transport and are replenished by abiotic deprotonation of  $\text{NH}_4^+$  ions (depending on the concentration gradient and pH), whereas nitrification and subsequent denitrification require additional reactions and are partly dependent on  $\text{NH}_3$  :  $\text{NH}_4^+$  availability (although see Zhu-Barker *et al.*, 2015 regarding  $\text{N}_2\text{O}$  production from other N species). Based on our empirical observations, we conclude that gaseous  $\text{NH}_3$  transport and biotic  $\text{NH}_3\text{-N}$  acquisition may be relevant both in managed systems, such as agricultural fields fertilized with N-rich amendments, and in unmanaged systems, where natural organic matter or atmospheric deposition can be transformed into gaseous  $\text{NH}_3$ .

### Abiotic edaphic properties influence subsurface $\text{NH}_3\text{-N}$ efflux, transport, and uptake

Our work supports previous findings that abiotic variables mediate  $\text{NH}_3$  efflux from soil (McCalley & Sparks, 2008; Kim & Or, 2019; Pelster *et al.*, 2019). In particular, alkaline pH favors  $\text{NH}_3$  gas efflux (Fig. 4a). This is not surprising, since the  $\text{pK}_a$  of  $\text{NH}_3$  is 9.2. We observed a strong relationship between soil pH and  $\text{NH}_3$  efflux despite considerable variation in mineralogy, organic matter content, and microbial activity in the soils that we incubated. Still, we found that substantial  $\text{NH}_3$  efflux is possible in non-alkaline environments, as observed from the most acidic sample included in our incubation (pH 2.52, Fig. 4a). The C content and net  $\text{CO}_2$  efflux from this soil were also high, suggesting that high microbial activity may support  $\text{NH}_3$  efflux even when other edaphic factors do not. It is also possible that  $\text{NH}_3$  efflux from this soil and other neutral or acidic soils is partly due to microscale pH heterogeneity, which we did not capture with our bulk soil pH measurements but has been linked to emission of pH-dependent nitrogenous gases (Kim & Or, 2019). Soil clay content was negatively

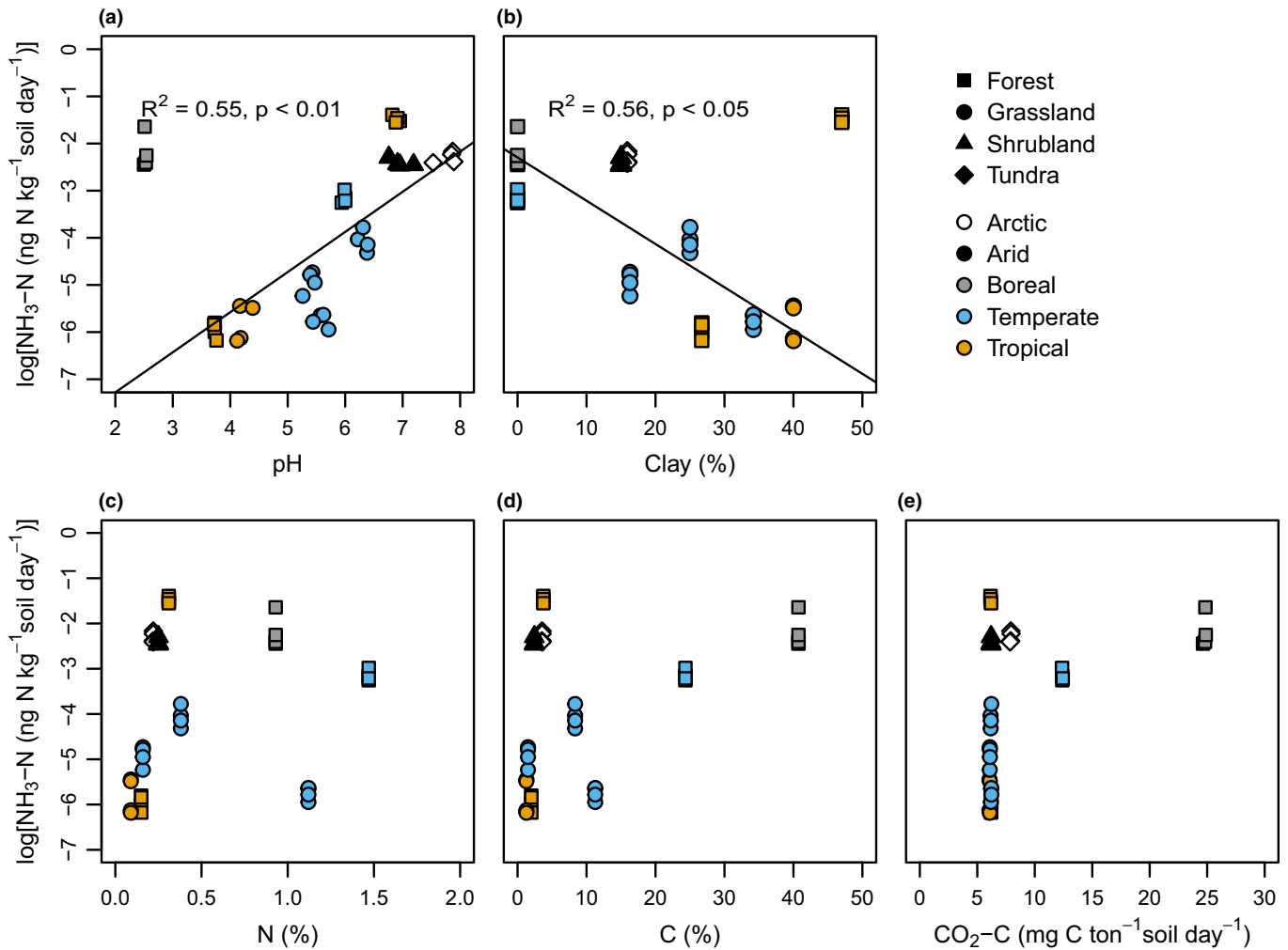


**Fig. 4** Relationship between  $\text{NH}_3\text{-N}$  efflux and edaphic properties. (a)  $\text{NH}_3\text{-N}$  efflux from incubated soils was positively associated with soil pH ( $y = 0.85$  (pH)  $- 8.98$ ,  $R^2 = 0.55$ ,  $F = 16.33$ ,  $P < 0.01$ , excluding values from an organic forest soil horizon with a pH of 2.5). (b)  $\text{NH}_3\text{-N}$  efflux was negatively associated with soil clay content ( $y = -0.09$ (% clay)  $- 2.30$ ,  $R^2 = 0.56$ ,  $F = 11.78$ ,  $P < 0.05$ ; excluding values from a forest topsoil with a clay content of 47%). (c–e)  $\text{NH}_3\text{-N}$  efflux was not significantly correlated with soil N content, C content, or  $\text{CO}_2\text{-C}$  respiration. Soils originating from forests, grasslands, a desert shrubland, and a tundra are represented by squares, circles, triangles, and diamonds, respectively. Soils originating from arctic, arid, boreal, temperate, and tropical climates are represented by white, black, gray, blue, and orange symbols, respectively ( $n = 4$  replicates per location).

associated with  $\text{NH}_3$  efflux. Our work does not determine to what extent this is related to differences in gas movement through pore networks of coarse- vs fine-textured soils, or geochemical interactions between  $\text{NH}_3$  molecules and minerals that dominate soils with different textures. Another limitation of our laboratory-scale incubation is that it does not represent a wide variety of soil depths or depth-related  $\text{NH}_3$  dynamics. Interestingly, even soil collected from a horizon 1 m below the surface released a considerable quantity of  $\text{NH}_3$  (Fig. S7; Table S2). Although this deeper soil horizon may not typically experience conditions similar to those imposed in our incubation, these results show that it is possible for deep soil N to be transformed into  $\text{NH}_3$  gas that can move and be intercepted by plants or microbes before it is released to the atmosphere, adsorbed, or otherwise lost or transformed. Future work should investigate these processes across a greater range of soil depths, types, and environmental conditions (such as temperature and moisture) to determine how edaphic properties

and environmental conditions influence the quantity of  $\text{NH}_3$  available for subsurface transport and biological assimilation by plants and microbes.

In addition to mediating total  $\text{NH}_3$  efflux from natural soil, pH is a strong mediator of subsurface  $\text{NH}_3$  transport and subsequent availability for plant or microbial uptake. The absence of  $^{15}\text{N}$  in plants separated from a  $^{15}\text{NH}_3$  source by an acidic substrate in our three-compartmented mesocosms (Figs 1, S3–S5) suggests that upon reaching the acidic substrate, the  $^{15}\text{NH}_3$  was protonated into  $^{15}\text{NH}_4^+$  and did not move through this substrate into the compartment containing the plant roots and fungal hyphae. Plants grown in mesocosms with neutral or alkaline substrate separating them from the  $^{15}\text{NH}_3$  source took up significantly more  $^{15}\text{N}$ , suggesting that the  $^{15}\text{NH}_3$  diffused laterally through the substrate into the plant compartment, where it was taken up either by roots or mycorrhizal hyphae that transferred  $^{15}\text{N}$  to the plant. Because appreciable quantities of  $^{15}\text{N}$



were neither detected in plants grown in mesocosms that did not receive an injection of  $^{15}\text{NH}_3$  nor in plants grown with a pH 4 substrate separating them from the  $^{15}\text{NH}_3$  source, we concluded that plants that acquired  $^{15}\text{N}$  did so primarily through subsurface uptake pathways rather than uptake through aerial tissues. Furthermore, higher  $^{15}\text{N}$  enrichment of root and hyphal tissues compared to the shoot tissues is also consistent with a subsurface N acquisition pathway following a pulse of  $^{15}\text{NH}_3$  gas (Fig. S5). Notably, plant  $^{15}\text{N}$  uptake was significantly enhanced even at pH 7, indicating that  $\text{NH}_3$  can move belowground even when bulk soil pH is neutral. The low moisture content, low nutrient content, and coarse texture of the subsurface substrate likely facilitated gaseous  $\text{NH}_3$  transport and uptake. Additional experiments are necessary to evaluate the extent to which  $\text{NH}_3$  transport and biotic uptake are inhibited by soil moisture, nutrient, or clay content.

### Arbuscular mycorrhizal fungi facilitate plant nitrogen uptake from ammonia

Our work also shows that biotic associations with AM fungi facilitate plant acquisition of N that originates from  $\text{NH}_3$  gas. Previous work has shown that AM fungi improve plant N acquisition, but there is still considerable uncertainty regarding the magnitude of N acquired and the mechanisms through which AM fungi improve plant N acquisition (Hobbie *et al.*, 1999; Hodge *et al.*, 2001; Hodge & Fitter, 2010; Hobbie & Högberg, 2012; Nuccio *et al.*, 2013; Hodge & Storer, 2015). These studies document mycorrhizal N acquisition from  $\text{NH}_4^+$ ,  $\text{NO}_3^-$ , and organic sources. Here, we show that  $\text{NH}_3$  gas may also be an important

component of mycorrhizal resource exchange. It is not clear from our work whether greater  $\text{NH}_3\text{-N}$  assimilation by AM-colonized plants is due to enhanced  $\text{NH}_3\text{-N}$  uptake by the plant roots themselves or to N exchange between AM fungi and plants. Our work provides support for both pathways. The root systems of AM-colonized plants were larger than those of uncolonized plants (Fig. S1). In addition to facilitating the growth of a larger root system with which plants could acquire N directly, AM-driven changes in root cell physiology (such as the abundance of aquaporins – membrane proteins hypothesized to allow the passage of  $\text{NH}_3$ ) may also enhance root acquisition of  $\text{NH}_3\text{-N}$  (Maurel *et al.*, 2015; Jia-Dong *et al.*, 2019). Isotopic analysis of bulk root, shoot, and fungal tissues shows that the AM fungal tissue itself was more enriched in  $^{15}\text{NH}_3$ -derived N than the AM-colonized plant tissue (Fig. S5). This suggests that AM fungal acquisition of  $\text{NH}_3\text{-N}$  is efficient relative to plant acquisition of this N source, and that the fungus may be able to leverage this N acquisition capacity in exchange for plant photosynthates. Interestingly, although a partnership with AM fungi enhanced total plant  $\text{NH}_3\text{-N}$  acquisition, higher  $\delta^{15}\text{N}$  values in hyphal tissues compared to plant tissues suggests that the fungus retained a higher proportion of the  $\text{NH}_3\text{-N}$  during the short exposure time-frame. In comparison, when plants and AM fungi were exposed to  $\text{NH}_3$  released from organic matter decomposition over a several-month period, the proportional contribution of  $\text{NH}_3\text{-N}$  to total plant N was significantly lower for AM-colonized plants than for uncolonized plants (Fig. S6b). Taken together, these results indicate that plant and fungal  $\text{NH}_3\text{-N}$  acquisition and mycorrhizal exchange of  $\text{NH}_3$ -derived N can occur rapidly and contribute significantly to plant N nutrition, but that over a short

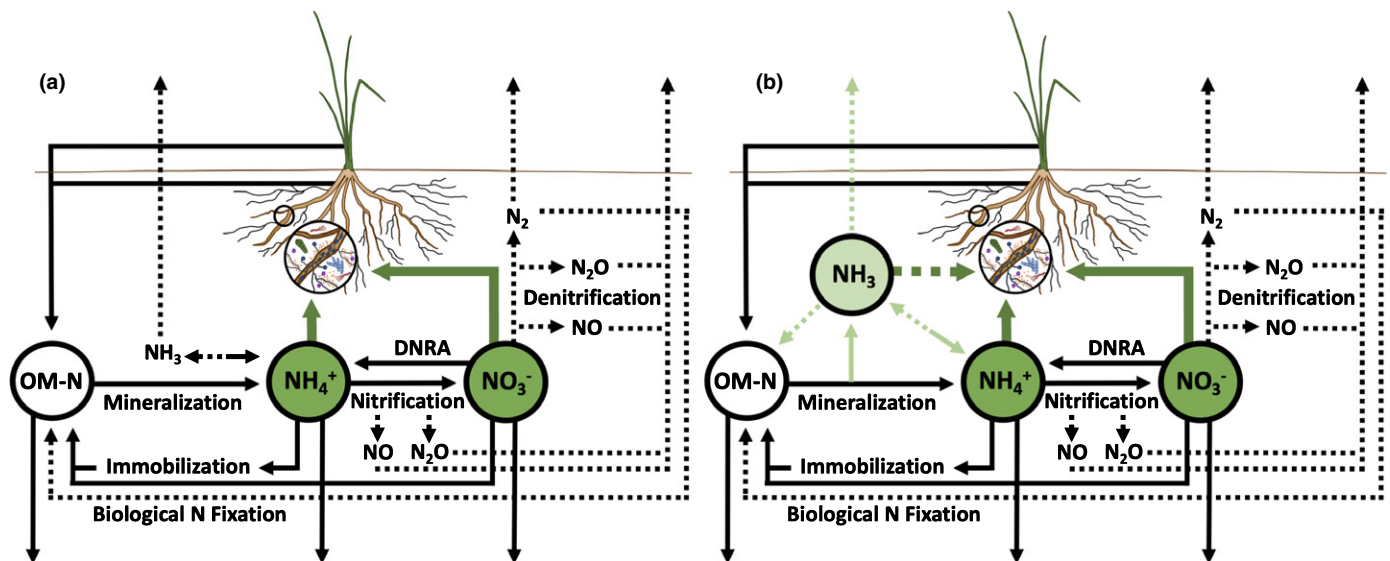


**Fig. 5** Primary subsurface nitrogen (N) transformations and transport pathways that influence plant and microbial inorganic N acquisition. Movement of ions and other nongaseous matter is represented with solid lines; movement of gaseous N species is represented by dashed lines. Dark green arrows represent pathways of plant or microbial N acquisition from inorganic N forms, which are highlighted in green circles. (a) Traditional subsurface models assume that  $\text{NO}_3^-$  and  $\text{NH}_4^+$  are the primary inorganic N species that non-N-fixing plants and microbes take up from the soil. (b) A revised subsurface model based on the work presented here includes  $\text{NH}_3$  gas as an additional inorganic N species that contributes to plant and microbial N acquisition belowground. Light green arrows highlight  $\text{NH}_3$  transport and transformation pathways. Because it is a gas,  $\text{NH}_3$  may travel on different timescales and in different directions than  $\text{NO}_3^-$  or  $\text{NH}_4^+$  ions.  $\text{NH}_3$  gas may also be taken up through different biological mechanisms. OM-N, organic matter nitrogen; DNRA, dissimilatory nitrate reduction.

period of time, the fungus first satisfies its own N demand. The presence of highly enriched AM hyphae supports the hypothesis that AM fungi could supply plants with  $\text{NH}_3\text{-N}$  and may be better able to acquire  $\text{NH}_3\text{-N}$  compared to roots. However, the heterogeneous enrichment of different hyphae indicates that some of the hyphae played a more active role in  $\text{NH}_3\text{-N}$  acquisition than others (Fig. 3). It is not clear from our data whether this is due to differences in hyphal viability, age, growth outside the root during  $\text{NH}_3$  exposure, different  $\text{NH}_3$  pathways, or other factors. Future research should continue to investigate drivers governing AM fungal N uptake and transfer to plants.

### Amending the soil nitrogen cycle

Based on these observations and the estimate that approximately one third of the Earth's soils have a pH of 7 or higher (Batjes, 2009; Slessarev *et al.*, 2016), we propose that conceptual models of the terrestrial N cycle should include subsurface  $\text{NH}_3$  production, transport, and associated N acquisition by plants and soil biota (Fig. 5).  $\text{NH}_3$  gas has a unique molecular structure that differentiates its reactivity, interactions with organic matter, spatial and temporal transport patterns, and potential biological uptake pathways from those of  $\text{NH}_4^+$  and  $\text{NO}_3^-$  ions or other soil N species currently included in conceptual subsurface N pools (Shi *et al.*, 2016; Weil & Brady, 2017; Hestrin *et al.*, 2019; Moreau *et al.*, 2019).  $\text{NH}_3$  gas may move more quickly than  $\text{NH}_4^+$ ,  $\text{NO}_3^-$ , and dissolved organic N, particularly under dry conditions. It is also capable of moving in all directions through nanoscale pore spaces belowground, whereas  $\text{NO}_3^-$  or organic N movement is more strongly influenced by convective transport in soil water. Furthermore, biological mechanisms for  $\text{NH}_3$  uptake, such as aquaporins or gaseous diffusion through membranes, may be different from those involved in uptake of  $\text{NH}_4^+$ ,  $\text{NO}_3^-$ , or organic molecules (Maurel *et al.*, 2015). Therefore, we think that it is worthwhile to consider  $\text{NH}_3$  gas pools and fluxes explicitly in studies of the terrestrial N cycle. It is worth noting that subsurface  $\text{NH}_3$  travel and uptake may be possible in other systems and should also be considered when interpreting the results of  $^{15}\text{N}$  tracer studies where a portion of the  $^{15}\text{N}$  tracer may also travel as  $^{15}\text{NH}_3$  gas. In addition to anhydrous  $\text{NH}_3$ , other agricultural amendments may be transformed into  $\text{NH}_3$  and play an important role in agricultural N cycling and plant nutrition. Our findings may also be relevant in unfertilized systems, where a portion of N assimilated by plants may originate from subsurface  $\text{NH}_3$  gas released from soil organic matter. Future research should investigate the prevalence and drivers of subsurface  $\text{NH}_3$  production, movement, and uptake (including competition between and transformation by soil biota), biological mechanisms for subsurface  $\text{NH}_3$  acquisition, and how these processes interact with the global N cycle.

### Acknowledgements





This work was supported in part by the Cornell Atkinson Center for Sustainability. RH acknowledges support from the NSF IGERT Program (DGE-0903371 and DGE-1069193), NSF-

BREAD (grant no. IOS-0965336; BMGF grant no. OPP51589), and the NSF GRFP (DGE-1144153). This research was also supported in part by the US Department of Energy Office of Biological and Environmental Research, Genomic Science Program LLNL Bioenergy Scientific Focus Area SCW1039. Work at LLNL was conducted under the auspices of DOE Contract DE-AC52-07NA27344. Special thanks to Akio Enders for help with experimental design, Kelly Hanley for help with sample collection, Kim Sparks and Cornell Stable Isotope Facility staff for help with IRMS analysis, Christina Ramon for help with NanoSIMS sample preparation, Maria Harrison for providing the plant and fungal germplasm, and Thea Whitman and Rhona Stuart for feedback on an earlier draft of the manuscript. The authors declare no competing financial interests.

### Author contributions

RH and JL conceived the experiments; RH performed the experiments and analyzed the data; PKW assisted with NanoSIMS data collection; PKW and JP-R assisted with NanoSIMS data interpretation; RH wrote the article; all authors contributed to the final draft.

### ORCID

Rachel Hestrin  <https://orcid.org/0000-0003-1315-8870>  
Johannes Lehmann  <https://orcid.org/0000-0002-4701-2936>  
Jennifer Pett-Ridge  <https://orcid.org/0000-0002-4439-2398>  
Peter K. Weber  <https://orcid.org/0000-0001-6022-6050>

### Data availability

The data that support the findings of this study are available in Cornell University's digital repository eCommons (Hestrin *et al.*, 2021). NanoSIMS data are available from the authors upon request.

### References

- Ahmed ZU, Woodbury PB, Sanderman J, Hawke B, Jauss V, Solomon D, Lehmann J. 2017. Assessing soil carbon vulnerability in the western USA by geospatial modeling of pyrogenic and particulate carbon stocks. *Journal of Geophysical Research-Biogeochemistry* 122: 354–369.
- Bates D, Maechler M, Bolker B, Walker S. 2015. Fitting linear mixed-effects models using lme4. *Journal of Statistical Software* 67: 1–48.
- Batjes NH. 2009. Harmonized soil profile data for applications at global and continental scales: updates to the WISE database. *Soil Use Management* 25: 124–127.
- Bouwman AF, Boumans LJM, Batjes NH. 2002. Estimation of global  $\text{NH}_3$  volatilization loss from synthetic fertilizers and animal manure applied to arable lands and grasslands. *Global Biogeochemical Cycles* 16: 8–1–8–14.
- Bouwman AF, Lee DS, Asman WAH, Dentener FJ, Van Der Hoek KW, Olivier JGJ. 1997. A global high-resolution emission inventory for ammonia. *Global Biogeochemical Cycles* 11: 561–587.
- Campbell SA, Vallano DM. 2018. Plant defences mediate interactions between herbivory and the direct foliar uptake of atmospheric reactive nitrogen. *Nature Communications* 9: 4743.
- Cayuela ML, Sánchez-Monedero MA, Roig A, Hanley K, Enders A, Lehmann J. 2013. Biochar and denitrification in soils: when, how much and why does biochar reduce  $\text{N}_2\text{O}$  emissions? *Scientific Reports* 3: 1732.

- Chalk P, Smith C. 2020. On inorganic N uptake by vascular plants: can  $^{15}\text{N}$  tracer techniques resolve the  $\text{NH}_4^+$  versus  $\text{NO}_3^-$  “preference” conundrum? *European Journal of Soil Science* 2020: 1–18.
- Chapin FS, Moilanen L, Kielland K. 1993. Preferential use of organic nitrogen for growth by a non-mycorrhizal arctic sedge. *Nature* 361: 150–153.
- Ciais P, Sabine C, Bala G, Bopp L, Brovkin V, Canadell J, Chhabra A, DeFries R, Galloway J, Heimann M *et al.* 2013. Carbon and other biogeochemical cycles. In: Stocker TF, Qin D, Plattner GK, Tignor M, Allen SK, Boschung J, Nauels A, Xia Y, Bex V, Midgley PM, eds. *Climate Change 2013: The Physical Science Basis. Contribution of Working Group I to the Fifth Assessment Report of the Intergovernmental Panel on Climate Change*. Cambridge, UK: Cambridge University Press.
- Dawson GA. 1977. Atmospheric ammonia from undisturbed land. *Journal of Geophysical Research: Oceans and Atmospheres* 82: 3125–3133.
- Dentener FJ, Crutzen PJ. 1994. A three-dimensional model of the global ammonia cycle. *Journal of Atmospheric Chemistry* 19: 331–369.
- Dharmakeerthi RS, Hanley K, Whitman T, Woolf D, Lehmann J. 2015. Organic carbon dynamics in soils with pyrogenic organic matter that received plant residue additions over seven years. *Soil Biology & Biochemistry* 88: 268–274.
- Dijkstra FA, Morgan JA, Blumenthal D, Follett RF. 2010. Water limitation and plant inter-specific competition reduce rhizosphere-induced C decomposition and plant N uptake. *Soil Biology Biochemistry* 42: 1073–1082.
- Farquhar GD, Firth PM, Wetselaar R, Weir B. 1980. On the gaseous exchange of ammonia between leaves and the environment – determination of the ammonia compensation point. *Plant Physiology* 66: 710–714.
- Flechard CR, Massad RS, Loubet B, Personne E, Simpson D, Bash JO, Cooter EJ, Nemitz E, Sutton MA. 2013. Advances in understanding, models and parameterizations of biosphere–atmosphere ammonia exchange. *Biogeosciences* 10: 5183–5225.
- Fowler D, Coyle M, Skiba U, Sutton MA, Cape JN, Reis S, Sheppard LJ, Jenkins A, Grizzetti B, Galloway JN *et al.* 2013. The global nitrogen cycle in the twenty-first century. *Philosophical Transactions of the Royal Society B: Biological Sciences* 368: 20130164.
- Frisz Jf, Lou K, Klitzing Ha, Hanafin Wp, Lizunov V, Wilson RL, Carpenter KJ, Kim R, Hutcheon Id, Zimmerberg J *et al.* 2013. Direct chemical evidence for sphingolipid domains in the plasma membranes of fibroblasts. *Proceedings of the National Academy of Sciences, USA* 110: E613–E622.
- Galloway JN, Dentener FJ, Capone DG, Boyer EW, Howarth RW, Seitzinger SP, Asner GP, Cleveland CC, Green PA, Holland EA *et al.* 2004. Nitrogen cycles: past, present, and future. *Biogeochemistry* 70: 153–226.
- Galloway JN, Townsend AR, Erismann JW, Bekunda M, Cai Z, Freney JR, Martinelli LA, Seitzinger SP, Sutton MA. 2008. Transformation of the nitrogen cycle: recent trends, questions, and potential solutions. *Science* 320: 889–892.
- Ghosal S, Fallon S, Leighton T, Wheeler K, Hutcheon I, Weber PK. 2008. Analysis of bacterial spores using nano-secondary ion mass spectrometry (NanoSIMS). *Analytical Chemistry* 80: 5986–5992.
- Giovannetti M, Mosse B. 1980. An evaluation of techniques for measuring vesicular arbuscular mycorrhizal infection in roots. *New Phytologist* 84: 489–500.
- Gruber N, Galloway JN. 2008. An Earth-system perspective of the global nitrogen cycle. *Nature* 451: 293–296.
- Hestrin R, Hammer EC, Mueller CW, Lehmann J. 2019. Synergies between mycorrhizal fungi and soil microbial communities increase plant nitrogen acquisition. *Communications Biology* 2: 233.
- Hestrin R, Torres-Rojas D, Dynes J, Hook J, Regier T, Gillespie A, Smernik R, Lehmann J. 2019. Fire-derived organic matter retains ammonia through covalent bond formation. *Nature Communications* 10: 664.
- Hestrin R, Weber PK, Pett-Ridge J, Lehmann J. 2021. Data from: Plants and mycorrhizal symbionts acquire substantial soil nitrogen from gaseous ammonia transport. *eCommons* doi: 10.7298/q898-5m03.
- Hobbie EA, Högberg P. 2012. Nitrogen isotopes link mycorrhizal fungi and plants to nitrogen dynamics. *New Phytologist* 196: 367–382.
- Hobbie EA, Macko SA, Shugart HH. 1999. Interpretation of nitrogen isotope signatures using the NIFTE model. *Oecologia* 120: 405–415.
- Hodge A, Campbell CD, Fitter AH. 2001. An arbuscular mycorrhizal fungus accelerates decomposition and acquires nitrogen directly from organic material. *Nature* 413: 297–299.
- Hodge A, Fitter AH. 2010. Substantial nitrogen acquisition by arbuscular mycorrhizal fungi from organic material has implications for N cycling. *Proceedings of the National Academy of Sciences, USA* 107: 13754–13759.
- Hodge A, Storer K. 2015. Arbuscular mycorrhiza and nitrogen: implications for individual plants through to ecosystems. *Plant and Soil* 385: 1–19.
- Hong JJ, Park YS, Bravo A, Bhattarai KK, Daniels DA, Harrison MJ. 2012. Diversity of morphology and function in arbuscular mycorrhizal symbioses in *Brachypodium distachyon*. *Planta* 236: 851–865.
- van Hove LWA, Heeres P, Bossen ME. 2002. The annual variation in stomatal ammonia compensation point of rye grass (*Lolium perenne* L.) leaves in an intensively managed grassland. *Atmospheric Environment* 36: 2965–2977.
- Huygens D, Díaz S, Urcelay C, Boeckx P. 2016. Microbial recycling of dissolved organic matter confines plant nitrogen uptake to inorganic forms in a semi-arid ecosystem. *Soil Biology and Biochemistry* 101: 142–151.
- Jia-Dong H, Tao D, Hui-Hui W, Ying-Ning Z, Qiang-Sheng W, Kamil K. 2019. Mycorrhizas induce diverse responses of root TIP aquaporin gene expression to drought stress in trifoliolate orange. *Scientia Horticulturae* 243: 64–69.
- Johnson JE, Berry JA. 2013. The influence of leaf-atmosphere  $\text{NH}_3(\text{g})$  exchange on the isotopic composition of nitrogen in plants and the atmosphere. *Plant, Cell & Environment* 36: 1783–1801.
- Kim M, Or D. 2019. Microscale pH variations during drying of soils and desert biocrusts affect HONO and  $\text{NH}_3$  emissions. *Nature Communications* 10: 3944.
- Leigh J, Hodge A, Fitter AH. 2009. Arbuscular mycorrhizal fungi can transfer substantial amounts of nitrogen to their host plant from organic material. *New Phytologist* 181: 199–207.
- Liang B, Lehmann J, Solomon D, Kinyangi J, Grossman J, O'Neill B, Skjemstad JO, Thies J, Luizao FJ, Petersen J *et al.* 2006. Black carbon increases cation exchange capacity in soils. *Soil Science Society of America Journal* 70: 1719–1730.
- Mader P, Vierheilig S-E, Boller T, Frey B, Christie P, Wiemken A. 2000. Transport of  $^{15}\text{N}$  from a soil compartment separated by a polytetrafluoroethylene membrane to plant roots via the hyphae of arbuscular mycorrhizal fungi. *New Phytologist* 146: 155–161.
- Maurel B, Boursiac Y, Luu DT, Santoni V, Shazad Z, Verdoucq L. 2015. Aquaporins in plants. *Physiological Reviews* 95: 1321–1358.
- McCalley CK, Sparks JP. 2008. Controls over nitric oxide and ammonia emissions from Mojave Desert soils. *Oecologia* 156: 871–881.
- Moreau D, Bardgett RD, Finlay RD, Jones DL, Philippot L. 2019. A plant perspective on nitrogen cycling in the rhizosphere. *Functional Ecology* 33: 540–552.
- Mueller CW, Rethemeyer J, Kao-Kniffin J, Löppmann S, Hinkel KM, Bockheim JG. 2015. Large amounts of labile organic carbon in permafrost soils of northern Alaska. *Global Change Biology* 21: 2804–2817.
- Näsholm T, Ekblad A, Nordin A, Giesler R, Högberg M, Högberg P. 1998. Boreal forest plants take up organic nitrogen. *Nature* 392: 914–916.
- Nuccio EE, Hodge A, Pett-Ridge J, Herman DJ, Weber PK, Firestone MK. 2013. An arbuscular mycorrhizal fungus significantly modifies the soil bacterial community and nitrogen cycling during litter decomposition. *Environmental Microbiology* 15: 1870–1881.
- Pajares S, Bohannan BJM. 2016. Ecology of nitrogen fixing, nitrifying, and denitrifying microorganisms in tropical forest soils. *Frontiers in Microbiology* 7: 1045.
- Pelster DE, Watt D, Strachan IB, Rochette P, Bertrand N, Chantigny MH. 2019. Effects of initial soil moisture, clod size, and clay content on ammonia volatilization after subsurface band application of urea. *Journal of Environmental Quality* 48: 549–558.
- Phillips JM, Hayman DS. 1970. Improved procedures for clearing roots and staining parasitic and vesicular-arbuscular mycorrhizal fungi for rapid assessment of infection. *Transactions of the British Mycological Society* 55: 158–161.
- Potter C, Klooster S, Krauter C. 2003. Regional modeling ammonia emissions from native soil sources in California. *Earth Interactions*. 7: 1–28.
- R Development Core Team. 2011. *R: A language and environment for statistical computing*. [WWW document] URL <http://www.R-project.org/>.

- Recha JW, Lehmann J, Walter MT, Pell A, Verchot L, Johnson M. 2012. Stream discharge in tropical headwater catchments as a result of forest clearing and soil degradation. *Earth Interactions* 16: 1–18.
- Riedo M, Milford C, Schmid M, Sutton MA. 2002. Coupling soil–plant–atmosphere exchange of ammonia with ecosystem functioning in grasslands. *Ecological Modelling* 158: 83–110.
- Schjoerring JK, Husted S, Mäck G, Nielsen KH, Finneman J, Mattsson M. 2000. Physiological regulation of plant–atmosphere ammonia exchange. *Plant & Soil* 221: 95–102.
- Shi M, Fisher JB, Brzostek ER, Phillips RP. 2016. Carbon cost of plant nitrogen acquisition: global carbon cycle impact from an improved plant nitrogen cycle in the Community Land Model. *Global Change Biology* 22: 1299–1314.
- Slessarev EW, Lin Y, Bingham NL, Johnson JE, Dai Y, Schimel JP, Chadwick OA. 2016. Water balance creates a threshold in soil pH at the global scale. *Nature* 540: 567–569.
- Solomon D, Lehmann J, Kinyangi J, Pell A, Theis J, Riha S, Ngoze S, Amelung W, Preez C, Machado S *et al.* 2009. Anthropogenic and climate influences on biogeochemical dynamics and molecular-level speciation of soil sulfur. *Ecological Applications* 19: 989–1002.
- Sparks JP, Monson RK, Sparks KL, Lerdau M. 2001. Leaf uptake of nitrogen dioxide (NO<sub>2</sub>) in a tropical wet forest: implications for tropospheric chemistry. *Oecologia* 127: 214–221.
- Stein L, Klotz MG. 2016. The nitrogen cycle. *Current Biology* 26: R94–R98.
- Sutton MA, Reis S, Riddick SN, Dragosits U, Nemitz E, Theobald MR, Tang YS, Braban CF, Vieno M, Dore AJ *et al.* 2013. Towards a climate-dependent paradigm of ammonia emission and deposition. *Philosophical Transactions of the Royal Society B: Biological Sciences* 368: 20130166.
- Thomen A, Robert F, Remusat L. 2014. Determination of the nitrogen abundance in organic materials by NanoSIMS quantitative imaging. *Journal of Analytical Atomic Spectrometry* 29: 512–519.
- Vitousek PM, Howarth RW. 1991. Nitrogen limitation on land and in the sea: how can it occur? *Biogeochemistry* 13: 87–115.
- Weil RR, Brady NC. 2017. Nitrogen and sulfur economy of soils. In: Weil RR, Brady NC, eds. *The nature and properties of soils, 15<sup>th</sup> edn*. Upper Saddle River, NJ, USA: Pearson, 601–642.
- Whitman T, Zhu ZH, Lehmann J. 2014. Carbon mineralizability determines interactive effects on mineralization of pyrogenic organic matter and soil organic carbon. *Environmental Science & Technology* 48: 13727–13734.
- Zackrisson O, Nilsson MC, Wardle DA. 1996. Key ecological function of charcoal from wildfire in the Boreal forest. *Oikos* 77: 10–19.
- Zhu Q, Riley WJ, Tang J, Koven CD. 2016. Multiple soil nutrient competition between plants, microbes, and mineral surfaces: model development, parameterization, and example applications in several tropical forests. *Biogeosciences* 13: 341–363.
- Zhu-Barker X, Cavazos AR, Ostrom NE, Horwath WR, Glass JB. 2015. The importance of abiotic reactions for nitrous oxide production. *Biogeochemistry* 126: 251–267.

## Supporting Information

Additional Supporting Information may be found online in the Supporting Information section at the end of the article.

**Fig. S1** Total plant biomass (dry weight).

**Fig. S2** Total plant N uptake.

**Fig. S3** Percent of total plant N derived from NH<sub>3</sub>.

**Fig. S4** Estimated proportion of daily plant N uptake from subsurface NH<sub>3</sub>-N.

**Fig. S5** <sup>15</sup>N enrichment of fungi and plants following <sup>15</sup>NH<sub>3</sub> injection through acid, neutral, and alkaline subsurface substrates.

**Fig. S6** Total and proportional plant <sup>15</sup>N acquisition from subsurface gas produced during organic matter (OM) decomposition.

**Fig. S7** Variation in NH<sub>3</sub>-N efflux from natural soils.

**Table S1** ANOVA table for the relationship between pH, mycorrhizal colonization, and plant <sup>15</sup>N derived from <sup>15</sup>NH<sub>3</sub>.

**Table S2** Characteristics of natural soils used in laboratory incubation.

Please note: Wiley Blackwell are not responsible for the content or functionality of any Supporting Information supplied by the authors. Any queries (other than missing material) should be directed to the *New Phytologist* Central Office.